Journal of Glaciology, Vol. 50, *No.* 168, 2004

Genesis of dewatering structures and its implications for melt-out till identification

ANDERS E. CARLSON*
Department of Geology and Geophysics, University of Wisconsin–Madison, Wisconsin 53706, U.S.A.
E-mail: carlsand@geo.oregonstate.edu

ABSTRACT. Dewatering structures are a common feature used to identify melt-out till, and the lack of such structures in till could preclude deposition by melt-out. To assess the conditions under which melt-out till can be deposited without forming dewatering structures, I use geotechnical data and a quasi-two-dimensional model of geothermal melt-out. Critical discharge determined from geotechnical data suggests that low-hydraulic-conductivity till can transport up to 1.3 m^3 water $a^{-1}\,m^{-2}$ without forming dewatering structures, which is two to three orders of magnitude greater than the volume of meltwater produced at the base of glaciers. The model indicates that debris content of the ice and the ability of the till to drain govern effective pressure during melt-out. If the drainage system is poorly developed or the till comes from debris-poor ice, effective pressure is below zero, the condition under which dewatering structures could form. However, till from relatively debris-rich ice (>40% debris) with a well-developed drainage system (channels every 10 m) can dewater without forming dewatering structures. This suggests that the lack of dewatering structures in till does not necessarily imply deposition by lodgement or deforming bed.

INTRODUCTION

Observations of recently deposited melt-out till have shown that till dewatering can distort, sort or alter sediment when sediment liquefies and is transported upwards, leaving identifiable dewatering structures that indicate deposition by melt-out (Boulton, 1970, 1971; Lawson, 1979). The presence of these dewatering structures has been used to identify Pleistocene-age melt-out till (Boulton, 1971; Drozdowski, 1983; Shaw, 1983; Piotrowski and others, 2001), while the lack of these structures could imply deposition by a process other than melt-out (Alley, 1991; Johnson and Hansel, 1999). However, melt-out till can also be deposited without these structures forming (Boulton, 1970; Lawson, 1979; Ham and Mickelson, 1994), confusing the genetic characteristics of melt-out till. From a review of the properties of melt-out till, it can be concluded that deposition by melt-out could be inferred if the till is stratified (e.g. containing sorted layers) because the removal of ice and dewatering can be detected (Shaw, 1979; Haldorsen and Shaw, 1982). The presence of these sorted layers facilitates dewatering and does not resolve the genetic characteristics of structureless till. Because of this ambiguity, the lack of structures in homogeneous till requires further investigation (Alley, 1991).

Genetic interpretations of till have broader consequences for inferences of glacier dynamics and climate. The genesis of southern Laurentide ice sheet till has implications for both the motion of the southern Laurentide ice lobes (e.g. basal sliding or subglacial bed deformation) and its attendant effects on climate change during retreat from the Last Glacial Maximum (reviewed by Clark and others, 1999). However, interpretation of Pleistocene deposits is usually restricted to exposures in sediment, making genetic inferences difficult in those areas with few exposures such as the southern margin of the Laurentide ice sheet (Mickelson and others, 1983; Johnson and Hansel, 1999). Thus, a better understanding of the structures associated with various till types is required if limited observations in exposures are to be extrapolated to an entire lobe. To help resolve the ambiguity in till characteristics, I use calculations and model results of melt-out scenarios to provide a quantitative assessment of the factors that control the formation of dewatering structures during melt-out.

CRITICAL DISCHARGE METHODS

The formation of dewatering structures is dependent on the interplay between water delivery to the till and water expulsion from till (Fig. 1) (Boulton and Paul, 1976). Water in the till drains slowly following the hydraulic gradient, i (unitless) (see Table 1 for symbol key). The addition of more water to the till than can be expelled eventually increases porewater pressure in the till, u (kN m^{-2}), in excess of the opposing total pressure, P (kN m^{-2}), and the critical hydraulic gradient, i_c (unitless), is reached. Effective pressure, Pe (kN m^{-2}), is then below zero,

$$\mathrm{Pe} = P - u \qquad (1)$$

(the hydraulic gradient is greater than the critical hydraulic gradient), and grains can be transported upward by water, forming dewatering structures (Coduto, 1999).

*Present address: Department of Geosciences, Oregon State University, 104 Wilkinson Hall, Corvallis, Oregon 97331, U.S.A.

https://doi.org/10.3189/172756504781830358 Published online by Cambridge University Press

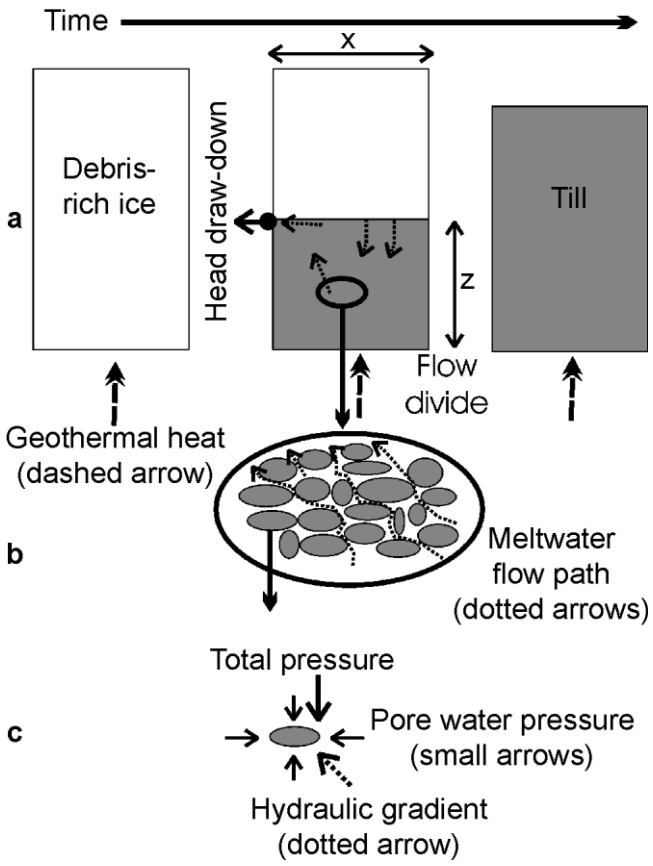

Fig. 1. A cartoon depicting the melt-out system used in both discharge calculations and melt-out model. (a) A debris-rich block of ice melts from the bottom up due to geothermal heat (dashed arrows). Meltwater (dotted arrows) drains through the till towards a hydraulic-head drawdown at the ice–till interface (black dot and arrow). Eventually, all ice melts, leaving slightly overconsolidated till. Horizontal half-space, x (m), and vertical till thickness, z (m), are indicated. (b) Meltwater (dotted arrows) flows through the pore space of the till. If more water is added to the till than can drain out, pore-water pressure increases. If pore-water pressure exceeds total pressure because the till is incapable of draining all the water added, then dewatering structures can form. (c) Individual stress distribution on a single grain. Total pressure (large arrow and downward-pointed small arrow) is the combined pressure of till, ice and meltwater above the grain. Pore-water pressure (small arrows) is isotropic, while the hydraulic gradient (dotted arrow) is towards the hydraulic-head drawdown.

Table 1. A list and description of the symbols used in the text. Units are excluded where dimensionless

Symbol	*SI units*	*Description*
A	m^2	Area
c		Degree of consolidation
e		Void ratio
Gs		Specific gravity
h	m	Head
h_w	$m\,a^{-1}$	Additional water
i		Hydraulic gradient
i_c		Critical hydraulic gradient
k	$m\,a^{-1}$	Hydraulic conductivity
Mr	$m\,a^{-1}$	Melt rate
n		Porosity
n_f		Final porosity
n_i		Initial porosity
P	$kN\,m^{-2}$	Total pressure
Pe	$kN\,m^{-2}$	Effective pressure
Q	$m^3\,a^{-1}$	Discharge
S		Saturation
t	years	Time
u	$kN\,m^{-2}$	Pore-water pressure
Vs	$m\,a^{-1}$	Seepage velocity
x	m	Half-space
z	m	Total till thickness
γ_d	$kN\,m^{-3}$	Dry unit weight
γ_i	$10\,kN\,m^{-3}$	Unit weight of ice
γ_s	$kN\,m^{-3}$	Saturated unit weight
γ_w	$9.81\,kN\,m^{-3}$	Unit weight of water
ω		Moisture content

To determine the discharge (expulsion) at the critical hydraulic gradient, the critical seepage velocity, Vs ($m\,a^{-1}$), is first calculated, which is the maximum velocity at which water can move through the sediment without pore-water pressure exceeding total pressure:

$$\mathrm{Vs} = k i_c\,, \tag{2}$$

where k ($m\,a^{-1}$) is hydraulic conductivity (Coduto, 1999). The discharge, Q ($m^3\,a^{-1}$), at the critical seepage velocity is determined over a $1\,m^2$ area, A (m^2).

$$Q = \mathrm{Vs}A\,. \tag{3}$$

If the discharge at the critical seepage velocity is greater than the volume of water supplied by basal melting from geothermal heat, water drains through the pore spaces and no dewatering structures will form. If the discharge is less than the volume of meltwater supplied, effective pressure will be below zero and dewatering structures can form. These calculations of the discharge at the critical hydraulic gradient apply to any gradient direction; however, the hydraulic gradient is assumed to be towards a hydraulic-head drawdown at the ice–till interface (Fig. 1).

To determine the critical hydraulic gradient, moisture contents, ω (unitless), were converted into saturated unit weights, γ_s ($kN\,m^{-3}$), following Coduto (1999).

$$e = \omega \mathrm{Gs}/S\,, \tag{4}$$

where e (unitless) is void ratio, S (unitless) is saturation and Gs (unitless) is the specific gravity of the till.

$$\gamma_d = \mathrm{Gs}\gamma_w/(e+1)\,, \tag{5}$$

where γ_d ($kN\,m^{-3}$) is the dry unit weight, γ_w ($9.81\,kN\,m^{-3}$) is the unit weight of water and

$$\gamma_s = \gamma_d(1+\omega)\,. \tag{6}$$

With a known saturated unit weight, the critical hydraulic gradient is determined,

$$i_c = (\gamma_s - \gamma_w)/\gamma_w\,. \tag{7}$$

The geotechnical data used in these calculations are from Kewaunee Formation till of eastern Wisconsin, which has a mean constituent make-up of 21% sand, 43% silt and 36% clay (Le Roy, 1992; Carlson, 2002). With its relatively high clay content, this till represents a fine-grained end-member, making this a conservative calculation of till dewatering. The till contains few clasts, and clast size ranges from <0.5 to ~10 cm. The Kewaunee till has sharp contacts with the underlying till and gravel, and shows no evidence of gradation, zone of mixing or plowing into the underlying sediment (Carlson, 2002). Critical discharge was deter-

https://doi.org/10.3189/172756504781830358 Published online by Cambridge University Press

Table 2. Calculation of the critical hydraulic gradient using moisture contents of 105–121 and specific gravities of 2.65–2.70. Average critical hydraulic gradient is calculated with 1 standard deviation

ω	i_c (Gs = 2.65)	i_c (Gs = 2.70)
105	0.436	0.443
106	0.433	0.440
119	0.397	0.404
121	0.392	0.398
Average (1 std dev.)	0.41 (0.02)	0.42 (0.02)
Combined average (1 std dev.)	0.42 (0.02)	

Table 3. Calculation of discharge at the critical hydraulic gradient using hydraulic conductivities of 2.9–3.8 m a^{-1} and specific gravities of 2.65–2.70. A calculation is also made using a hydraulic conductivity of 0.0038 m a^{-1}, which is three orders of magnitude less than the hydraulic conductivity of Kewaunee till

k	Vs (Gs = 2.65)	Vs (Gs = 2.70)	Average Vs	Q
m a^{-1}	m a^{-1}	m a^{-1}	m a^{-1}	m^3 a^{-1} m^{-2}
2.9	12.6	12.9	12.8	1.3
3.8	16.3	16.6	16.5	1.6
0.0038	0.0163	0.0166	0.0165	0.0016

mined from the geotechnical properties of this clayey till measured by Earth Tech, Inc. (Le Roy, 1992). Earth Tech, Inc. calculated hydraulic conductivity in the field, using the baildown and slug-test methods, and moisture content and grain-size in the laboratory. Hydraulic conductivity ranged between 2.9 and 3.8 m a^{-1}. Moisture content in samples from below the water table (to insure 100% saturation) varied between 105 and 121 (unitless) (Le Roy, 1992). The till is assumed to have a specific gravity of 2.65–2.70 (unitless) in accord with clay-rich materials (Coduto, 1999).

CRITICAL DISCHARGE RESULTS

The saturated unit weight of the till was determined for known moisture contents and estimated specific gravities (Equations (4–6)). The unit weights vary between 13.7 and 14.2 kN m^{-3}, which result in critical hydraulic gradients of 0.39–0.44 (Equation (7); Table 2). The average between the two specific gravities and moisture contents determines a critical hydraulic gradient of approximately 0.42, which produces critical seepage velocities of 12.6–16.6 m a^{-1} (Equation (2); Table 3). Discharge at the critical seepage velocity over a 1 m^2 area is 1.3–1.6 m^3 water a^{-1} m^{-2} for the lower and upper limit of the hydraulic conductivity (averaged between Gs 2.65 and 2.70) (Equation (3); Table 3). If basal, geothermally melted ice constitutes the only water input into the system, these discharges for the Kewaunee till can be compared to known basal geothermal melt rates to ascertain if dewatering structures might be present.

The assumed specific gravity and possible inaccuracy in hydraulic conductivity introduce an unknown degree of error in these calculations. However, there is little variation in the specific gravity of clay-rich materials, and the range used here (2.65–2.70) covers this variability (Coduto, 1999). It is harder to assess the error involved with the hydraulic conductivity. The discharge calculated with these hydraulic conductivities is relatively high for clay-rich sediment, which may reflect non-uniformity in Kewaunee till (e.g. the presence of high-permeability layers in the till). A similar series of calculations was made with hydraulic conductivity three orders of magnitude lower to demonstrate the large degree of error that must be involved in the measurement of hydraulic conductivity to negate these calculations (Table 3). However, because of these assumptions, these results should be viewed as an order-of-magnitude value.

MELT-OUT MODEL METHODS

Because the geotechnical properties of the till reflect the modern field conditions and not the conditions during melt-out, a quasi-two-dimensional basal, debris-rich ice-melting model was developed to better understand the effects of debris content, drainage, consolidation, time and melt rate on effective pressure, hydraulic gradient and the mechanism of dewatering. The model uses basic laws of soil mechanics (see Coduto, 1999) and considers a half-space (the distance between regularly spaced channels at the ice–till interface and water-flow divide) of stagnant, debris-covered ice at the pressure-melting point overlying homogeneous saturated till (Fig. 1) (Boulton, 1970; Lawson, 1979; Shaw, 1979). Geothermal heat melts the block of ice from the bottom up, and this meltwater is the only water input into the system. All the meltwater enters the till and drains through the pore space of the till, following the hydraulic gradient. The presence of channels creates a hydraulic-head drawdown at the ice–till interface (Boulton, 1970; Shaw, 1979), forcing an oblique hydraulic gradient towards the channel. The till is initially considered normally consolidated to slightly underconsolidated because ice occupied the pore spaces when thick, active glacial ice overlaid the area. Slightly underconsolidated till transfers some of the total pressure to the pore water, which dissipates through time as the water drains and the till consolidates. After all ice has melted, normal consolidation to slight overconsolidation should characterize melt-out till. The purpose of the model is to conceptually determine under what conditions effective pressure will fall below zero during melt-out and dewatering structures can form. It does not include all the complexities of subglacial groundwater flow and the marginal glacial environment.

Pore-water pressure (isotropic) in the model results from meltwater added to the till flowing due to the hydraulic gradient, i (unitless), and part of the weight of the overlying till and ice. The hydraulic gradient is determined from the change in hydraulic head, $\mathrm{d}h/\mathrm{d}t$ (m a^{-1}), in the till and the distance over which the hydraulic head is lost: the vertical thickness of till, z (m).

$$z = \mathrm{Mr}t - [\mathrm{Mr}t(c - c/t)] \tag{8}$$

with a constant melt rate

$$\mathrm{d}h/\mathrm{d}t = 0.9\mathrm{Mr} + 0.9\mathrm{Mr}(x^2/2) \tag{9}$$

$$i = (\mathrm{d}h/\mathrm{d}t)/(\mathrm{d}z/\mathrm{d}t)\,, \tag{10}$$

where t (years) is time since the ice block began to melt, c is

https://doi.org/10.3189/172756504781830358 Published online by Cambridge University Press

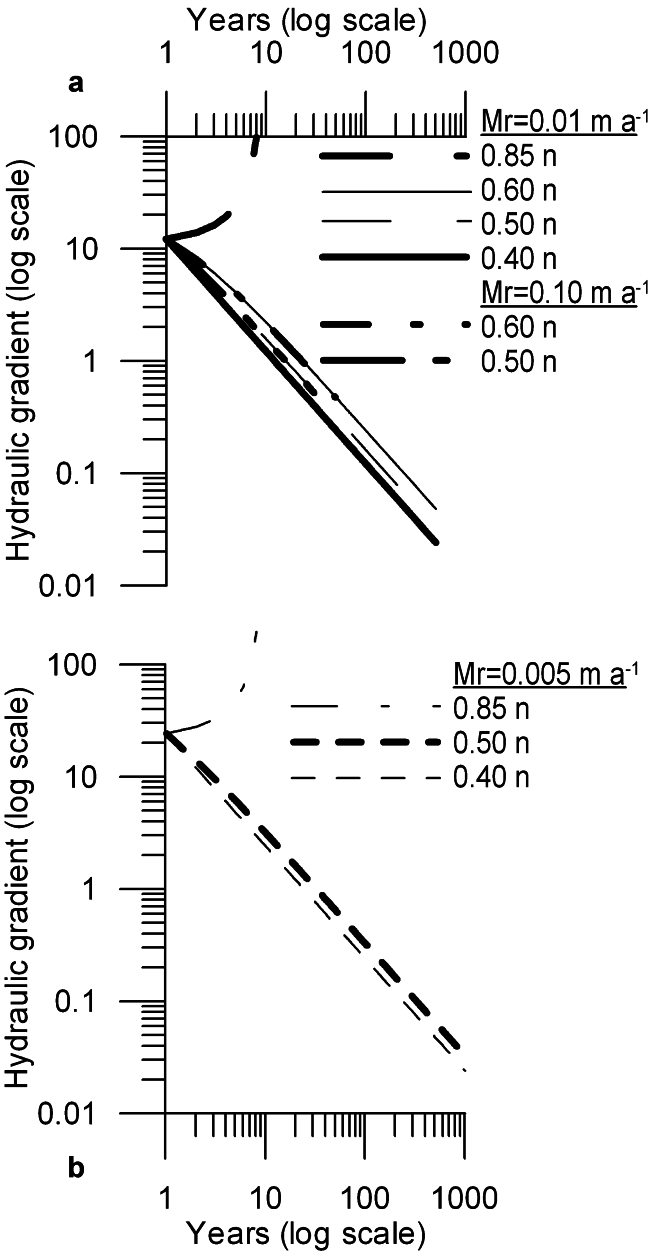

Fig. 2. Hydraulic gradient (unitless) through time (ice thickness = 5 m, half-space = 5 m). Melt rate and porosity (0.40–0.85) were varied to determine their control over the system. (a) Melt rate is 0.01 m a^{-1}. (b) Melt rate is 0.005 m a^{-1}. An order-of-magnitude greater melt rate of 0.10 m a^{-1} for porosity of 0.5–0.6 is included in (a).

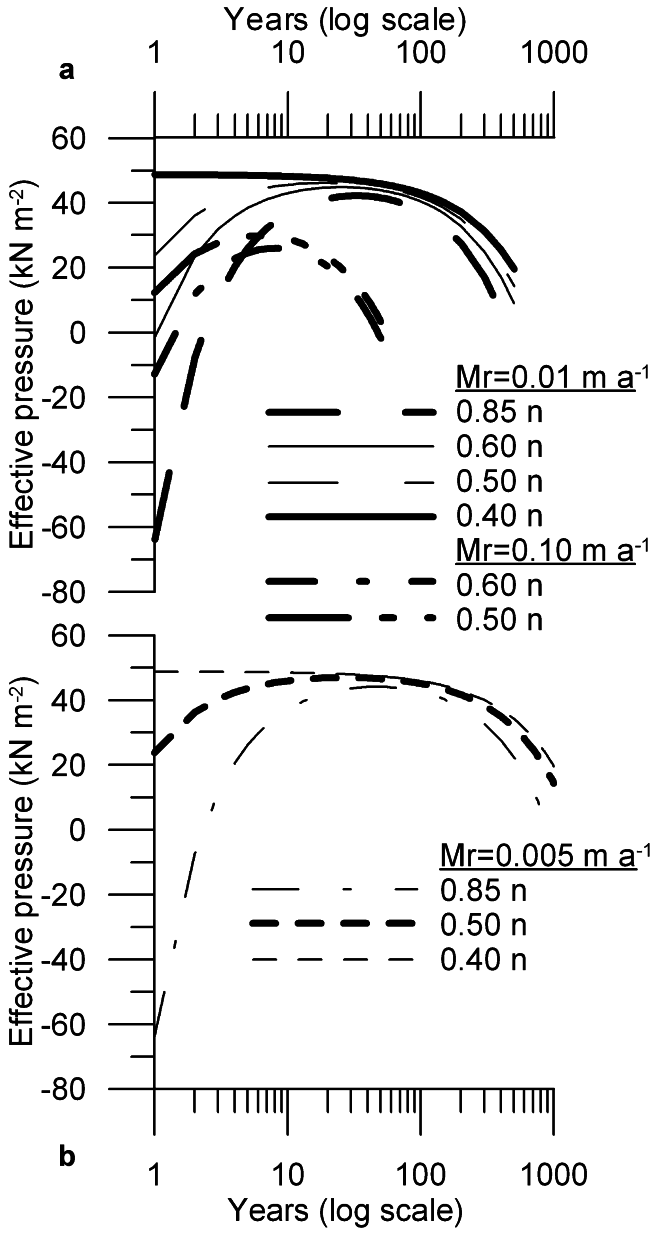

Fig. 3. Effective pressure (kN m^{-2}) through time (ice thickness = 5 m, half-space = 5 m). Porosity (0.40 and 0.85) and melt rate were varied to determine their control on the system. (a) Melt rate is 0.01 m a^{-1}. (b) Melt rate is 0.005 m a^{-1}. An order-of-magnitude greater melt rate of 0.10 m a^{-1} for porosity of 0.5–0.6 is included in (a).

degree of consolidation (unitless) = $(n_i - n_f)/n_f$ (n_i is initial porosity and n_f is final porosity (unitless), of the till, Mr (m a^{-1}) is melt rate, and x (m) is the half-space of the stagnant ice block (half the distance between channels: the distance between a channel and flow divide (Fig. 1)). Equation (8) determines the thickness of the till (first term) adjusted for consolidation (second term, c). The $c - c/t$ term (unitless) is empirical and modifies till thickness for time-varying consolidation which exponentially decreases through time (Coduto, 1999). Equation (9) calculates the vertical contribution of meltwater to the change in head (first term) and the integrated addition of meltwater across the half-space (x) (from the flow divide to the channel) (modified from Fountain, 1994), adding a quasi-second dimension to the model. The half-space controls the ability of the till to drain because increased distance to a channel increases the hydraulic head. Effective pressure is then calculated by Equation (1), with total pressure and pore-water pressure determined by:

$$P = \gamma_i(z_i - \mathrm{Mr}t)(1 - c/t) + \gamma_s(z)(1 - c/t) \quad (11)$$

$$u = \gamma_w(z + iz) + \gamma_i(z_i - \mathrm{Mr}t)[1 - (1 - c/t)] + \gamma_s(z)[1 - (1 - c/t)], \quad (12)$$

where γ_i (10 kN m^{-3}) is the unit weight of debris-rich ice, γ_s (14 kN m^{-3}) is the unit weight of the till from the previous section, and γ_w (9.81 kN m^{-3}) is the unit weight of water. The first and second terms of Equation (11) calculate the weight of ice and sediment supported by the till, respectively. The first term of Equation (12) determines the pore-water pressure from overlying water and the hydraulic gradient, while the second and third terms calculate the pressure from overlying ice and sediment supported by the pore

https://doi.org/10.3189/172756504781830358 Published online by Cambridge University Press

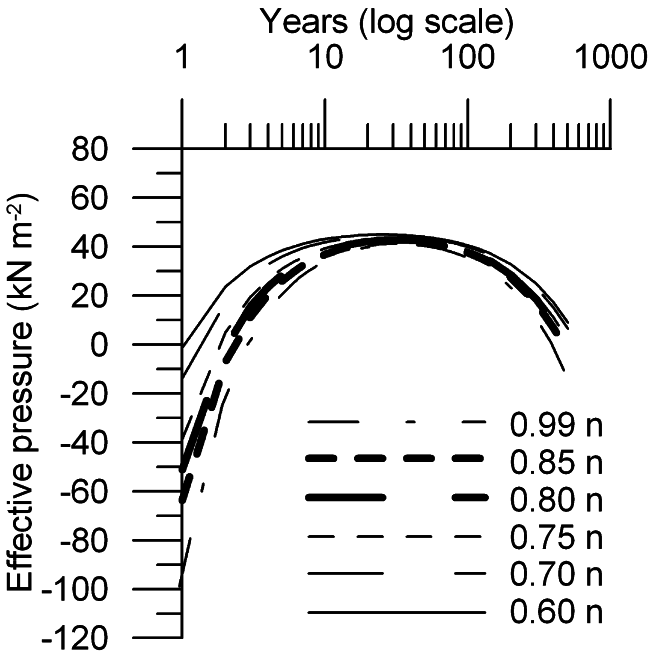

Fig. 4. Effective pressure ($kN\,m^{-2}$) with a constant melt rate of 0.01 m a^{-1} (ice thickness = 5 m, half-space = 5 m). Porosity is varied between 0.60 and 0.99 to determine at what debris content ($1-n$) effective pressure falls below zero.

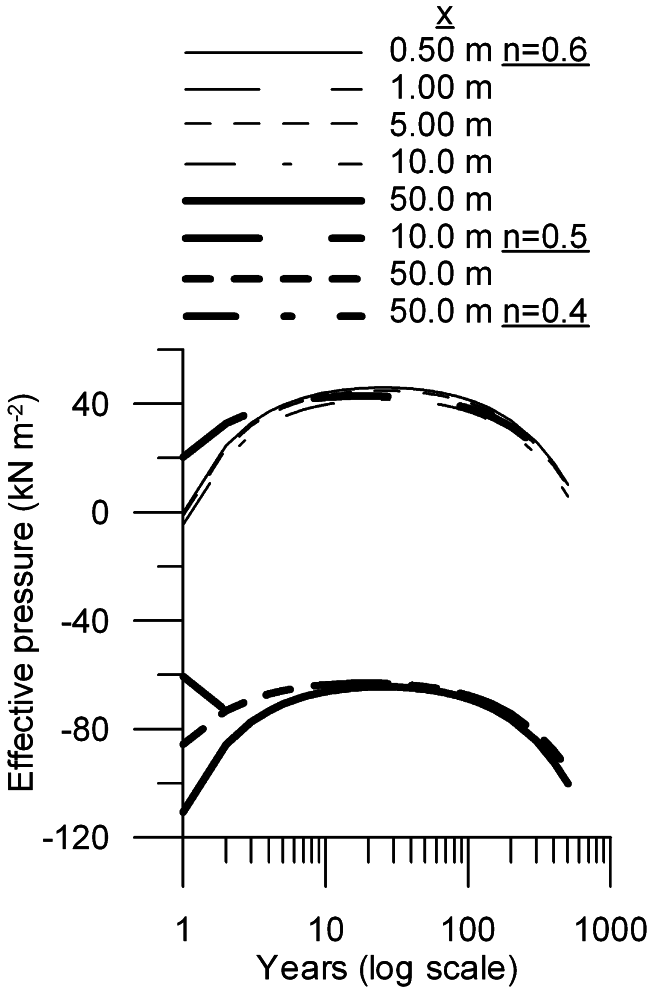

Fig. 5. Effective pressure ($kN\,m^{-2}$) with varied distance between channels (half-space = 0.50–50.0 m) and porosity (0.40–0.60).

water, respectively. The empirical $1-c/t$ term (unitless) partitions total pressure between pore water and sediment. As the model advances, grains consolidate due to the total pressure, the water drains, and the sediment assumes more of the total pressure. The till is allowed to completely consolidate to a final porosity (n_f) of 0.40 which is typical of modern melt-out till (Boulton and Paul, 1976; Ronnert and Mickelson, 1992).

The initial porosity (n_i) of the till needs to be determined to calculate the degree of consolidation, which should be equivalent to the debris content of the melting ice (debris content = $1-n$) (Ronnert and Mickelson, 1992). Measurements of the debris content of basal, debris-rich ice range between 1% and 74% debris (e.g. Lawson, 1979; Ronnert and Mickelson, 1992; Kirkbride, 1995). A range of debris contents is used in the model between 1% and 60% (initial porosity 0.99–0.40), spanning much of the modern variability. The half-space between channel and water-flow divide (x) also needs to be ascribed, and is usually between <5 and 180 m (Boulton, 1970; Shaw, 1979; Fountain, 1994; Engelhardt and Kamb, 1997; Fleming and Clark, 2000). A range in half-space is considered from 0.50 to 50 m, which is applicable to melt-out conditions (Boulton, 1970; Shaw, 1979; Carlson, 2002). Two initial debris-rich ice thicknesses, 5 and 10 m, are arbitrarily chosen, while a range of melt rates between 0.005 and 0.01 m a^{-1} is used, which covers most geothermal melt rates (Paterson, 1994). A third rate of 0.10 m a^{-1} is also used to test the sensitivity of the model to rapid melting.

MODEL RESULTS

Varying melt rate (0.10–0.005 m a^{-1}) (Figs 2 and 3), ice thickness (5–10 m) (not shown), porosity (0.99–0.40) (Fig. 4) and half-space (0.50–50 m) (Fig. 5) determined the sensitivity of the model to these inputs (Equations (1) and (8–12)). Thicker ice increases the time required to melt the ice at a given melt rate but does not affect the hydraulic gradient, and initial hydraulic gradients are the same (a 5 m block of ice is used in the following results). Higher melt rates increase the amount of meltwater added to the system, increasing the hydraulic gradient and pore-water pressure and decreasing the effective pressure. This effect only becomes appreciable at melt rates an order of magnitude greater (e.g. 0.10 m a^{-1}). In runs with moderate-to-low porosities, hydraulic gradients decrease through the melt period until all ice has melted (Fig. 2). However, at high initial porosities (e.g. 0.85n), the model is unstable and the hydraulic gradient increases rapidly. This is due to the large amount of consolidation the till must undergo to reach a final porosity of 0.40, which transfers much of the initial overburden to the pore water, increasing the hydraulic gradient. Increasing channel half-space also increases the hydraulic gradient (not shown), decreasing effective pressure (Fig. 5). These tests suggest that porosity and channel half-spacing have a greater effect on model predictions than melt rate and ice thickness, because they influence the degree of consolidation and ability of the till to drain.

During a model run, effective pressure (Equations (1), (11) and (12)) initially increases, becomes relatively constant, and then decreases towards the end of a run. This pattern represents initially rapid consolidation, followed by the interplay of sediment addition to the system and ice melting

https://doi.org/10.3189/172756504781830358 Published online by Cambridge University Press

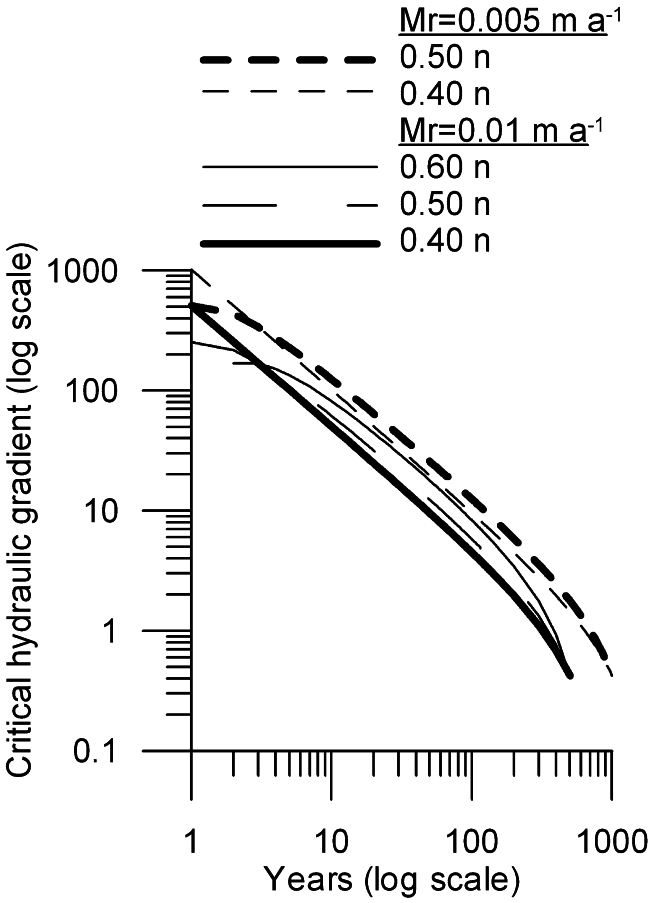

Fig. 6. Critical hydraulic gradient (unitless) with porosity varied between 0.40 and 0.60 and melt rate between 0.005 and 0.01 m a^{-1} (ice thickness = 5 m; channel half-space = 5 m).

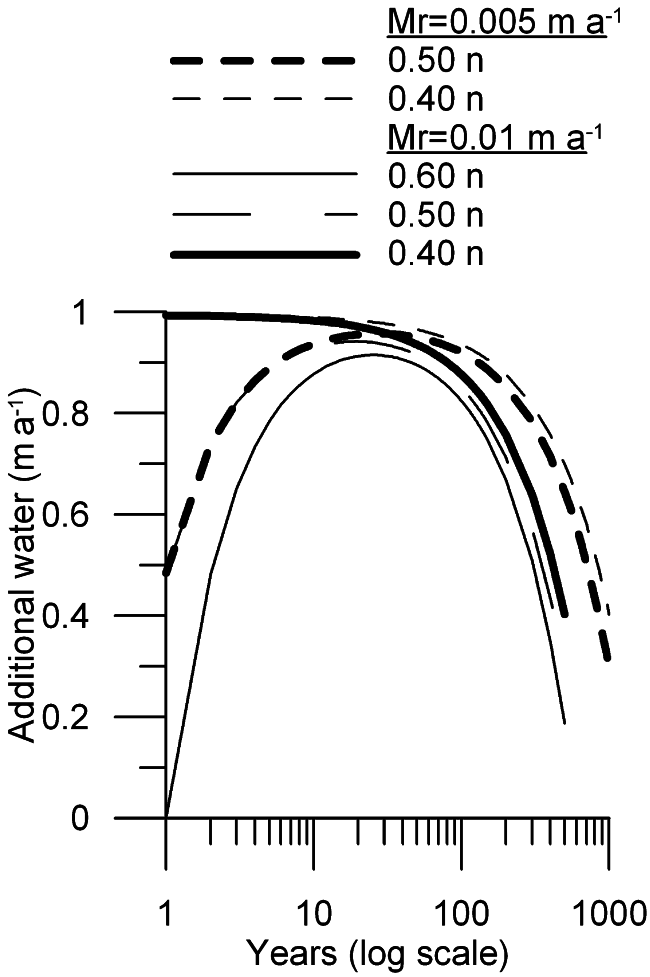

Fig. 7. The additional amount of water (m a^{-1}) required to increase pore-water pressure in excess of total pressure with porosity varied between 0.4 and 0.6 and melt rate between 0.005 and 0.01 m a^{-1} (ice thickness = 5 m, half-space = 5 m).

and the eventual removal of the overlying ice block. At initial porosities >0.60 (debris contents <40%), effective pressure is below zero for at least the early part of melt-out (Figs 3 and 4). With a more rapid melt rate (0.10 m a^{-1}), this initial porosity decreases closer to 0.50. Effective pressure is also sensitive to the half-space between the channel and water-flow divide. Increasing the half-space (e.g. from 5 to 10 m) decreases effective pressure, and at large half-spaces (e.g. 50 m) even decreasing initial porosity to 0.40 (no consolidation) does not raise effective pressure above zero (Fig. 5).

From these results, the critical hydraulic gradient through time is determined by setting total pressure equal to pore-water pressure and solving for the hydraulic gradient. Critical hydraulic gradients are initially extremely high, but drop to 0.42 during a model run (Fig. 6). This is due to the weight of the overlying ice block which is removed by melt-out, decreasing the critical hydraulic gradient.

The amount of additional water, hw (m a^{-1}), needed per year per half-space to reduce effective pressure below zero is calculated by dividing the critical hydraulic gradient by till thickness and subtracting out the meltwater input:

$$\mathrm{hw} = (i_c/z - \mathrm{d}h/\mathrm{d}t)/x. \qquad (13)$$

The amount of external water required mimics effective pressure (half-space = 5 m) and is initially between 0 and 1 m a^{-1} (porosity of 0.40 and 0.60, respectively), before increasing and subsequently decreasing during a model run (Fig. 7). Till from ice with an initial porosity >0.60 does not require additional water to form dewatering structures since effective pressure is already below zero.

These results are dependent on several assumptions necessary to construct the model. The model assumes that all meltwater enters the till, and does not account for meltwater initially lost to a channel or water film at the ice–till interface. Any loss of water, though, would decrease the amount of water added to the till, decreasing pore-water pressure. This would facilitate melt-out till deposition without the formation of dewatering structures, and makes the model conservative because it simulates an end-member state. Also, the model only includes water added from geothermal melting and not from groundwater or surficial meltwater penetrating to the till. The effects of this additional water depend on its amount (Fig. 7) which may or may not be great enough to decrease effective pressure below zero. The heat-flux direction is not considered in the model. However, the model applies an oblique hydraulic gradient which would transport geothermal heat upward and along the ice–till interface, continuing basal melting. The flow of water through the pore spaces would also create frictional heat from water impacting grains, which would increase the amount of basal melting. This additional meltwater is disregarded in the model, and the amount needed to cause dewatering structures in till from debris-rich ice is likely greater than the amount that frictional heating could melt (Fig. 7). In addition, uniform debris-rich ice, not stratified

https://doi.org/10.3189/172756504781830358 Published online by Cambridge University Press

Table 4. The volume of water produced by basal melting for valley glaciers and ice sheets. Geothermal melt rates from Svalbard and Alaska were measured; the melt rates for the Saalian ice sheet and most glacier beds are estimates

Location	Geothermal heat	Melt rate	Volume of water	Source
	$J\,cm^2\,a^{-1}$	$m\,a^{-1}$	$m^3\,a^{-1}\,m^{-2}$	
Svalbard	167	0.01	0.009	Boulton (1970)
Burroughs Glacier, Alaska, U.S.A.		0.005	0.0045	Mickelson (1973)
Matanuska Glacier, Alaska, U.S.A.	211	0.0068	0.0061	Lawson (1979)
Saalian ice sheet		0.02	0.018	Boulton and others (1993)
~all glacier beds		0.01	0.009	Paterson (1994)

debris-rich ice, is used in the model. However, the model simulates deposition of massive melt-out till while melt-out till from stratified ice would likely show evidence of being deposited by melt-out (Lawson, 1979; Haldorsen and Shaw, 1982). Finally, till is assumed to completely consolidate during melt-out, which may not be the case in field conditions. If melt-out ended while some of the total pressure was still supported by pore water, consolidation would continue until the till had consolidated to accommodate the overburden.

DISCUSSION

Previous studies have calculated melt rates for valley glaciers (Boulton, 1970; Mickelson, 1973; Lawson, 1979) and estimated melt rates for ice sheets (Boulton and others, 1993; Paterson, 1994) (Table 4). These suggest meltwater production rates two to three orders of magnitude lower than the maximum discharge that can flow through the pore space of Kewaunee till (Table 3). If only geothermal heat melted basal ice from the bottom up, dewatering structures would not form, because water could flow through the pore space of the till without building up to the critical hydraulic gradient where effective pressure is below zero. However, if the hydraulic conductivity of the Kewaunee till is in error by three orders of magnitude, dewatering structures could form (Table 3). Otherwise, to produce dewatering structures, melt rates must be at least two orders of magnitude greater or have outside water added to the till.

The model results suggest that the debris content of the melting ice (initial porosity) and drainage distance (half-space) play an important role in the formation of dewatering structures. With a relatively high debris content (at least 40% debris), and closely spaced drainage system ($<$10 m half-space), melt-out till can dewater without forming dewatering structures. At lower debris contents, the initial pore space is too large for the till to support the overburden, and pore water assumes much of this pressure. This reduces effective pressure below zero, and dewatering structures can form. Greater spacing between channels can also reduce effective pressure below zero because increased spacing increases the amount of water added to the till that drains towards a specific channel, decreasing the ability of the till to drain. At half-spaces near 10 m, this effect can be canceled by increased debris content of the ice. However, at larger half-spaces approaching 50 m, the till cannot drain even with high debris contents, and dewatering structures will likely form.

Observations of melt-out deposition have suggested controls on dewatering structure formation (debris content and drainage) similar to those in the model (Boulton, 1970; Lawson, 1979; Ham and Mickelson, 1994). Dewatering structures will not form if the melt-out till comes from relatively debris-rich ice with a well-developed drainage system. However, the lower limit of debris content may be 20–30% debris (Lawson, 1979), which is 10–20% less than the model predicts. This suggests that the channel spacing in the model may be too great. Smaller channel spacing would be in better agreement with the smaller spacing of remnant channels observed in Pleistocene and modern melt-out till (Boulton, 1970; Shaw, 1979; Carlson, 2002) relative to the spacing under active glaciers and ice streams (Fountain, 1994; Engelhardt and Kamb, 1997). Including a water film at the ice–till interface in the model would also reduce the amount of water entering the till, rectifying model predictions and observations. This discrepancy suggests that the model predictions are conservative relative to actual melt-out conditions.

When the till comes from relatively debris-rich ice and can drain, geothermal heat produces insufficient meltwater to form dewatering structures, and an additional source of water is needed, which depends on the debris content of the ice and on the channel spacing. At 40% debris content and 5 m half-space, no additional water is needed, while greater debris contents and smaller half-spaces increase the amount of water needed (Fig. 7). A faster melt rate (e.g. 0.10 $m\,a^{-1}$) could also produce this additional water, but this is an order of magnitude greater than most geothermal melt rates (Table 4) and contradicts field observations of debris-covered, stagnant ice existing up to thousands of years. Alternatively, common processes at glacier margins, such as surface meltwater penetrating into the till, a rise in the groundwater table or upward groundwater flow, could introduce this additional water into the till (Piotrowski, 1997).

Because of the wide range in the debris content of basal ice and the local variability in ground and surface water flow at glacier margins, there should be a high degree of spatial variability in melt-out till where dewatering structures could form at one location but not at another. This variability should be considered when interpreting till genesis in areas with limited exposures, because the exposure may not be representative of the glacier/lobe scale and the lack of dewatering structures in an exposure does not preclude melt-out as the depositional process. This suggests that a better understanding of the spatial variability in marginal glacial environments is needed to improve interpretations of ice dynamics in areas with limited exposures of glacial till.

CONCLUSIONS

While geotechnical data indicate that low-hydraulic-conductivity till can dewater without forming dewatering structures, model predictions demonstrate that the melt-out process is more complicated. Dewatering structures may not form in melt-out till if the till comes from relatively debris-rich ice and has a well-developed drainage system.

https://doi.org/10.3189/172756504781830358 Published online by Cambridge University Press

However, if the ice has a low debris content or the till cannot drain, dewatering structures could form. This suggests that the lack of dewatering structures in till does not necessarily need to be explained by a lodgement or deforming-bed genesis, but the conditions for this may be relatively specific and require an improved understanding of basal and subglacial environments.

ACKNOWLEDGEMENTS

The author would like to thank T. Hooyer and the Quaternary Research Group of the Department of Geology and Geophysics, University of Wisconsin–Madison, for discussion and comments on these ideas. The contribution of data by Earth Tech, Inc. was vital to this research and much appreciated. Earlier drafts of the manuscript were improved by comments from D. Mickelson, B. Laabs, B. Swanson and M. Blair. In addition, comments by two anonymous reviewers were very helpful in finalizing the manuscript. Finally, the author would like to thank M. Sturm and N. Glasser for editorial help and additional suggestions.

REFERENCES

Alley, R. B. 1991. Deforming-bed origin for southern Laurentide till sheets? *J. Glaciol.*, **37**(125), 67–76.

Boulton, G. S. 1970. On the deposition of subglacial and melt-out tills at the margins of certain Svalbard glaciers. *J. Glaciol.*, **9**(56), 231–245.

Boulton, G. S. 1971. Till genesis and fabric in Svalbard. *In* Goldthwait, R.P., *ed. Till: a symposium*. Columbus, OH, Ohio State University Press, 41–72.

Boulton, G. S. and M. A. Paul. 1976. The influence of genetic processes on some geotechnical properties of glacial tills. *Q. J. Eng. Geol.*, **9**(3), 159–194.

Boulton, G. S., T. Slot, K. Blessing, P. Glasbergen and K.van Gijssel. 1993. Deep circulation of groundwater in overpressured subglacial aquifers and its geological consequences. *Quat. Sci. Rev.*, **12**(9), 739–745.

Carlson, A. E. 2002. The Quaternary geology of southern Sheboygan County, Wisconsin. (M.Sc. thesis, University of Wisconsin Madison.)

Clark, P. U., R. B. Alley and D. Pollard. 1999. Northern Hemisphere ice-sheet influences on global climate change. *Science*, **286**(5442), 1104–1111.

Coduto, D. P. 1999. *Geotechnical engineering, principles and practices*. Upper Saddle River, NJ, Prentice Hall Publishing.

Drozdowski, E. 1983. Load deformations in melt-out till and underlying laminated till: an example from northern Poland. *In* Evenson, E.B., C. Schlüchter and J. Rabassa, *eds. Tills and related deposits: genesis/petrology/application/stratigraphy*. Rotterdam, A.A. Balkema, 119–124.

Engelhardt, H. and B. Kamb. 1997. Basal hydraulic system of a West Antarctic ice stream: constraints from borehole observations. *J. Glaciol.*, **43**(144), 207–230.

Fleming, S.W. and P. U. Clark. 2000. Investigation of water pressure transient beneath temperate glaciers using numerical groundwater flow experiments. *J. Quat. Sci.*, **15**(6), 567–572.

Fountain, A. G. 1994. Borehole water-level variations and implications for the subglacial hydraulics of South Cascade Glacier, Washington State, U.S.A. *J. Glaciol.*, **40**(135), 293–304.

Haldorsen, S. and J. Shaw. 1982. Problem of recognizing melt-out till. *Boreas*, **11**(3), 261–277.

Ham, N. R. and D. M. Mickelson. 1994. Basal till fabric and deposition at Burroughs Glacier, Glacier Bay, Alaska. *Geol. Soc. Am. Bull.*, **106**(12), 1552–1559.

Johnson, W. H. and A. K. Hansel. 1999. Wisconsin Episode glacial landscape of central Illinois: a product of subglacial deformation processes? *In* Mickelson, D. M. and J.W. Attig, *eds. Glacial processes: past and present*. Boulder, CO, Geological Society of America, 121–135. (Special Paper 337.)

Kirkbride, M. P. 1995. Processes of transportation. *In* Menzies, J., *ed. Modern glacial environments: processes, dynamics and sediments. Vol. 1. Glacial environments*. Oxford, etc., Butterworth–Heinemann, 261–292.

Lawson, D. E. 1979. Sedimentological analysis of the western terminus region of the Matanuska Glacier, Alaska. *CRREL Rep* 79-9.

Le Roy, B. J. 1992. Kohler Town Hill proposed landfill site feasibility study: hydraulic conductivity testing of 15 newly installed wells. SEC Donohue Project No. 19211.103. Technical Roport, Earth Tech Incorporated, Sheboygan, Wisconsin.

Mickelson, D. M. 1973. Nature and rate of basal till deposition in a stagnating ice mass, Burroughs Glacier, Alaska. *Arct. Alp. Res.*, **5**(1), 17–27.

Mickelson, D. M., L. Clayton, D. S. Fullerton and H.W. Borns, Jr. 1983. The Late Wisconsin glacial record of the Laurentide ice sheet in the United States. *In* Wright, H. E., Jr, *ed. Late-Quaternary environments of the United States. Volume 1*. Minneapolis, MN, University of Minnesota Press, 3–37.

Paterson, W. S. B. 1994. *The physics of glaciers. Third edition*. Oxford, etc., Elsevier.

Piotrowski, J. A. 1997. Subglacial groundwater flow during the last glaciation in north-western Germany. *Sediment. Geol.*, **111**(1–4), 217–224.

Piotrowski, J. A., D. M. Mickelson, S. Tulaczyk, D. Krzyszkowski and F.W. Junge. 2001. Were deforming subglacial beds beneath past ice sheets really widespread? *Quat. Int.*, **86**(1), 139–150.

Ronnert, L. and D. M. Mickelson. 1992. High porosity of basal till at Burroughs Glaciers, southeastern Alaska. *Geology*, **20**(9), 849–852.

Shaw, J. 1979. Genesis of the Sveg tills and Rogen moraines of central Sweden: a model of basal meltout. *Boreas*, **8**(4), 409–426.

Shaw, J. 1983. Forms associated with boulders in melt-out till. *In* Evenson, E. B., C. Schlüchter and J. Rabassa, *eds. Tills and related deposits: genesis/petrology/application/stratigraphy*. Rotterdam, A.A. Balkema, 3–12.

MS received 22 November 2002 and accepted in revised form 10 December 2003